JCTC Journal of Chemical Theory and Computation

Effect of the f-Orbital Delocalization on the Ligand-Field Splitting Energies in Lanthanide-Containing Elpasolites

Mohamed Zbiri,[†] Claude A. Daul,[†] and Tomasz A. Wesolowski*,[‡]

Département de Chimie, Université de Fribourg - 9, Chemin du Musée, Pérolles, CH-1700 Fribourg, Switzerland, and Département de Chimie, Université de Genève - 30, quai Ernest-Ansermet, CH-1211 Genève 4, Switzerland

Received February 1, 2006

Abstract: The ligand-field induced splitting energies of f-levels in lanthanide-containing elpasolites are derived using the first-principles universal orbital-free embedding formalism [Wesolowski and Warshel, *J. Phys. Chem.* **1993**, *97*, 8050]. In our previous work concerning chloroelpasolite lattice ($Cs_2NaLnCl_6$), embedded orbitals and their energies were obtained using an additional assumption concerning the localization of embedded orbitals on preselected atoms leading to rather good ligand-field parameters. In this work, the validity of the localization assumption is examined by lifting it. In variational calculations, each component of the total electron density (this of the cation and that of the ligands) spreads over the whole system. It is found that the corresponding electron densities remain localized around the cation and the ligands, respectively. The calculated splitting energies of f-orbitals in chloroelpasolites are not affected noticeably in the whole lanthanide series. The same computational procedure is used also for other elpasolite lattices (Cs_2NaLnX_6, where X=F, Br, and I)—materials which have not been fabricated or for which the ligand-field splitting parameters are not available.

1. Introduction

Lanthanide complexes offer potential applications in chemistry, physics, and other related areas.[1−13] Theoretical modeling of such complexes involves high-cost methods because of the role of electron correlation and the necessity of taking into account the effects of the environment of the f-elements.[14−29] Density-functional-theory methods based on the Kohn−Sham equations (KS-DFT) became standard tools in modeling large polyatomic systems.[30−32] In practice, KS-DFT calculations apply approximations to the exchange-correlation functional and the associated potential which are usually rather adequate. Typically, they lead to results of reasonable accuracy at computational cost which is significantly lower than that of traditional wave function-based methods. For some systems and/or properties, however, standard approximations face difficulties. As far as the f-elements are concerned, they lead to rather satisfactory results concerning structure, energetics, and vibrational properties[33−35] but lead sometimes to qualitatively wrong results as far as the details of the electronic structure are concerned.[36−41] Alternatively, following the spirit of the ligand-field theory, the orbitals of key interest can be obtained using the embedding strategy, in which only the lanthanide is described at the orbital level, whereas its environment is represented by some "effective embedding potential".[42−46] In this work, we apply the nonempirical embedding formalism[48] in which the embedded subsystem is described at the orbital-level, whereas its environment is characterized by the electron density (ρ_{II}). For a given ρ_{II}, the embedded orbitals ($\phi_{(I)i}$) used to construct the electron density of the subsystem under investigation ($\rho_I = \sum_{i=1}^{N_I} n_i^I |\phi_{(I)i}|^2$) are obtained from one-electron Kohn−Sham-like equations:[48]

$$\left[-\frac{1}{2}\nabla^2 + V_{\text{eff}}^{\text{KSCED}}[\vec{r},\rho_I,\rho_{II}]\right]\phi_{(I)i} = \epsilon_{(I)i}\phi_{(I)i} \qquad (1)$$

The superscript KSCED (Kohn−Sham Equations with Constrained Electron Density) is used to indicate the difference between the effective potential in eq 1 and that in the

* Corresponding author e-mail: Tomasz.Wesolowski@chiphy.unige.ch.

[†] Université de Fribourg - 9.

[‡] Université de Genève - 30.

10.1021/ct060035a CCC: $33.50
Published on Web 06/08/2006

Kohn−Sham formalism.[31] Fully variational variant of the above scheme, where instead of assuming some ρ_{II} it is obtained from a complementary embedding equation in which ρ_I and ρ_{II} exchange their roles, represents one of the possible practical realizations of the subsystem formulation of density functional theory by Cortona.[47] The total effective potential $V_{\text{eff}}^{\text{KSCED}}[\rho_I,\rho_{II},\vec{r}]$ can be conveniently split into two components: the Kohn−Sham effective potential for the isolated subsystem ($V^{\text{KS}}[\vec{r},\rho_I]$) and the remaining part representing the environment ($V_{\text{emb}}^{\text{eff}}[\vec{r},\rho_I,\rho_{II}]$) which reads

$$V_{\text{emb}}^{\text{eff}}[\vec{r},\rho_I,\rho_{II}] = \sum_{A_{II}} -\frac{Z_{AII}}{|\vec{r}-\vec{R}_{AII}|} + \int \frac{\rho_{II}(\vec{r}\,')}{|\vec{r}\,'-\vec{r}|} d\vec{r}\,' + \frac{\delta E_{\text{xc}}[\rho_I+\rho_{II}]}{\delta\rho_I} - \frac{\delta E_{\text{xc}}[\rho_I]}{\delta\rho_I} + \frac{\delta T_{\text{s}}^{\text{nad}}[\rho_I,\rho_{II}]}{\delta\rho_I} \quad (2)$$

where $T_{\text{s}}^{\text{nad}}[\rho_I,\rho_{II}] = T_{\text{s}}[\rho_I + \rho_{II}] - T_{\text{s}}[\rho_I] - T_{\text{s}}[\rho_{II}]$, and the functionals $E_{\text{xc}}[\rho]$ and $T_{\text{s}}[\rho]$ are defined in the Kohn−Sham formalism.[31] Neither $V^{\text{KS}}[\vec{r},\rho_I]$ nor $V_{\text{emb}}^{\text{eff}}[\vec{r},\rho_I,\rho_{II}]$ depend on the orbitals but only on the electron densities of the two subsystems.

The numerical solution of eq 1 proceeds by representing embedded orbitals as a linear combination of atom-centered basis functions ($\{\chi_i^I\}$ and $\{\chi_i^{II}\}$). In such a case, two types of expansion are of great practical relevance: the approximated one, in which only selected atom-centered functions are used in the construction of embedded orbitals, and another one, in which all available atom-centered functions are used. The first type of expansion is an approximation, and such calculations are labeled here by KSCED(m) following the convention of ref 49. It was used in our previously reported work on the ligand-field parameters of the f-levels of lanthanide cations in chloroelpasolites. It is referred to also as "monomolecular expansion". This type of expansion is obviously attractive computationally. Its drawback is, however, the absence of the terms of the $\chi_k^I(\boldsymbol{r})^*\chi_l^{II}(\boldsymbol{r})$ type in the expansion of the total electron density ($\rho_{\text{total}} = \rho_I + \rho_{II}$). This makes the cases with possible intersubsystem charge-transfer and/or covalency computationally unattractive because of the very slow convergence of the KSCED(m) results with the basis set.[50]

Our previous studies showed that the differences between ligand-field splitting energies derived from KSCED(m) calculations and deduced from experiment[52] were rather small (relative errors withing 10−20%).[53] Such errors are qualitatively smaller than the ones corresponding to calculations applying conventional Kohn−Sham calculations or electrostatic-only embedding.[53] Several factors contribute to the deviations from experimental data: the intrinsic errors in the applied approximation for the exchange-correlation effective potential, the use of the average-of-configuration reference state, errors in the applied approximation to the nonadditive kinetic energy effective potential, and the absence of the $\chi_k^I(\boldsymbol{r})^*\chi_l^{II}(\boldsymbol{r})$ terms.

In the present work, one among possible sources of deviations between the calculated and experimental parameters reported previously is investigated in detail. The effect of charge transfer and covalency is quantified by comparing the ligand-field splitting energies derived from the two types of KSCED embedding calculations which use either monomer or supermolecular expansion of both components of the total electron density (ρ_I and ρ_{II}). Following the convention of ref 49, the calculations using the supermolecular expansion are labeled by KSCED(s) in this work.

It is worthwhile to notice that the possibility for a complete delocalization of f-orbitals and charge transfer might either improve or worsen the calculated splitting energy. The worsening of the results would indicate that the applied approximate functionals in the embedding potential given in eq 2 are not adequate, and their flaws are exposed by adding more flexibility to the embedded orbitals. One of the key issues of this work is, therefore, the determination whether the good quality of the obtained previously KSCED-(m) results is due to the localization assumption. This assumption is no longer made in the present work. The possibility of the intersystem charge-flow exposes the possible flaws of the approximations used in the embedding potential given in eq 2 such as an artificial charge-leak from ligands to the cation.[51] Due to the variational character of the applied method, the use of more centers in the orbital expansion leads to the results which are closer to the basis set limit. It is especially important in view of the possible extension of the present studies toward modeling the complete spectra of lanthanide centers in solids. Such a task hinges, however, not only on a reliable description of the effect of the environment—the main issue of this work—but also on a proper representation of the electronic structure of the isolated cation.

2. Computational Details

Applications of eqs 1 and 2 in computer modeling rely on the approximations to the relevant functionals: $T_{\text{s}}^{\text{nad}}[\rho_I,\rho_{II}]$ and $E_{\text{xc}}[\rho]$. The used functionals approximate reasonably well the exact embedding potential of eq 2 in the case of small overlap between the electron densities ρ_I and ρ_{II}. The applied gradient-dependent approximation for $T_{\text{s}}^{\text{nad}}[\rho_I,\rho_{II}]$ was chosen based on dedicated numerical tests in the case of such pairs of ρ_I and ρ_{II},[49] which do no overlap significantly—a case relevant for the present studies.

The exchange-correlation component of the effective embedding potential given in eq 2 was approximated by means of the functional of Perdew and Wang (PW91).[54] The van Leeuwen-Baerends (LB94) exchange-correlation potential[55] was used to approximate the exchange-correlation component of $V^{\text{KS}}[\vec{r},\rho_I]$ in eq 1. This choice was motivated by the fact that one component of the system (ligands) is negatively charged, and such systems are not well described by means of the Kohn−Sham equations applying semilocal functionals. The orbital-free embedding potential given in eq 2 depends not only on the choice of the approximations used to evaluate its exchange-correlation- and kinetic-energy dependent components but also on the choice of the electron density ρ_{II}. All the reported numerical values were obtained from fully variational calculations in which both ρ_{II} and ρ_{II} are derived from the minimization of the total-energy bifunctional $E[\rho_I,\rho_{II}]$ in eq 2. Such a minimization is

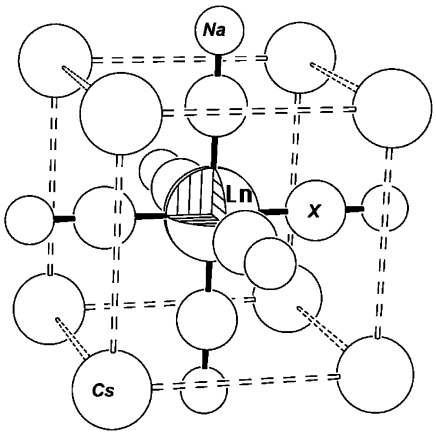

Figure 1. Schematic view on the environment of studied lanthanide cations. Each Ln^{3+} is hexacoordinated to six X^- ions (halides). The second coordinations sphere comprises eight Cs^+ ions at the corners of the cube. The third coordination sphere comprises six Na^+ ions occupying the vertices of the octahedron.

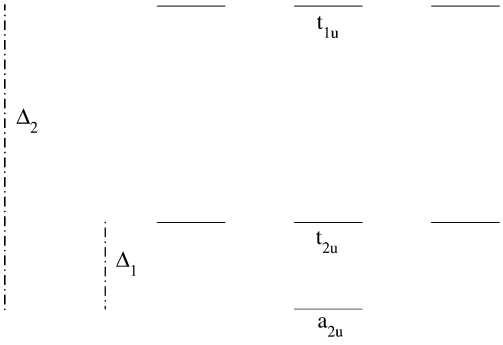

Figure 2. The f-orbital levels of Ln^{3+} in the octahedral environment.

performed by means of the "freeze-and-thaw" cycle of iterations described in ref 56.

The orbital-levels of an embedded lanthanide cation (Ln^{3+}) were obtained from eq 1 in which ρ_I corresponds to Ln^{3+} and ρ_{II} to the environment. The numerical implementation of eqs 1 and 2 into the Amsterdam Density Functional (ADF) package[60,61] was used in all calculations. Relativistic scalar ZORA,[57,58] all electron calculations were performed using the ZORA triple-ζ STO set plus one polarization function (ZORA/TZP).[59] Figure 1 shows the investigated system comprising the octahedral arrangement of the lanthanide cation Ln^{3+} and its ligands. O_h symmetry was assumed in all calculations.

Figure 2 shows the expected order of f-levels (a_{2u}, t_{2u}, and t_{1u}) and defines the two ligand-field splitting parameters Δ_1 and Δ_2. The energy levels were calculated for average-of-configuration, in which each f-orbital was partially occupied (occupation number (n/7)) for a given f^n configuration. The occupations of orbitals used to express the electron density of the ligands (ρ_{II}) were chosen in such a way that the corresponding single-determinantal wave function possesses the full symmetry of the system. In some cases (Ln=Ce, Pr, Nd, and Sm in Cs_2NaLnX_6), the orbitals of the ligands were maximaly filled (occupations given in Table. 1). The $N^{orb}A_{1.g}$ orbitals ($N^{orb} = 2$, 4, 7 and 8 corresponding to X=F, Cl, Br, and I in Cs_2NaLnX_6, respectively.) were, therefore, emptied.

Table 1: Electronic Occupation Numbers of the Hexahalide Anions for Each Irreducible Representation of the O_h Symmetry

irreps/halides	$(F^-)_6$	$(Cl^-)_6$	$(Br^-)_6$	$(I^-)_6$
$A_{1.g}$	6	10	16	22
$A_{2.g}$	0	0	2	4
E_g	12	20	36	52
$T_{1.g}$	6	12	24	36
$T_{2.g}$	6	12	30	48
$A_{2.u}$	0	0	2	4
E_u	0	0	4	8
$T_{1.u}$	24	42	72	102
$T_{2.u}$	6	12	30	48
$N_{electrons}$	60	108	216	324

3. Results and Discussion

This section comprises two parts. In the first one, the results of KSCED(s) and KSCED(m) calculations are compared in order to show the role of f-orbital delocalization on the calculated ligand-field splitting energies. The following section concerns the ligand-field splitting energies for a number of other elpasolites, for which either experimental ligand-field splitting were not accurately measured yet, or for materials which do not exist.

Table 2 collects the ligand-field splitting parameters Δ_1 and Δ_2 in lanthanide-containing chloroelpasolites $Cs_2NaLnCl_6$ derived from KSCED(m) and KSCED(s) calculations (see also Figure 3). Experimental results are also given for the sake of comparison. Note that the Δ_1 and Δ_2 values given in refs 40 and 53 for Yb (220 and 799 cm^{-1}, respectively) are erroneous, and we use the correct ones (301 and 747 cm^{-1}, respectively) here. In the whole lanthanide series, lifting the localization assumption for embedded orbitals does not affect significantly the calculated values of Δ_1. Both KSCED(m) and KSCED(s) results are very similar and agree very well with experiment. The experimental values of Δ_1 decrease almost monotonically in the whole series from 390 cm^{-1} (Ce) to 301 cm^{-1} (Yb). However, the dependence of the calculated values of Δ_1 on the number of f-electrons n_f is smoother than that deduced from experiment. The average and the maximal deviation from experimental data amount to 28 and 100 cm^{-1} (Sm) using the KSCED(m) scheme and 50 and 201 cm^{-1} (Ce) using KSCED(s), respectively. The corresponding mean absolute errors amount to 52 and 83 cm^{-1}.

Compared to Δ_1, the effect of lifting the localization assumption on Δ_2 is different. For cations with $n_f > 7$, the KSCED(m) and KSCED(s) values are almost identical. For $n_f < 7$ cations, the possibility of delocalization increases the calculated Δ_2 parameter by about 100 cm^{-1} bringing the calculated values closer to the experimental data.

The average and the maximal deviation from the experimental data amount to 178 and 320 cm^{-1} (Eu) for KSCED(m) and 141 and 315 cm^{-1} (Ho) for KSCED(s), respectively. The corresponding mean absolute errors amount to 100 and 168 cm^{-1}.

Table 2: Experimental and Calculated Ligand-Field Splitting Parameters Δ_1 and Δ_2 (in cm^{-1}) Derived from KSCED(s) and KSCED(m) Calculations[a]

		Ce	Pr	Nd	Pm	Sm	Eu	Gd	Tb	Dy	Ho	Er	Tm	Yb
experiment	Δ_1	390	462	343		250	341		349	345	358	300	299	301
	Δ_2	1072	1172	988		803	973		840	808	865	764	790	747
eq 2	Δ_1	591	536	480	445	434	410	351	341	319	315	303	294	290
KSCED(s)	Δ_2	1122	1006	896	830	825	716	641	621	570	550	530	519	503
eq 2	Δ_1	478	435	392	365	350	329	312	312	291	291	279	266	273
KSCED(m)	Δ_2	929	855	773	725	696	653	620	629	576	577	553	528	537

[a] Calculations were made at the ab initio optimized[63] ion−ligand distances.

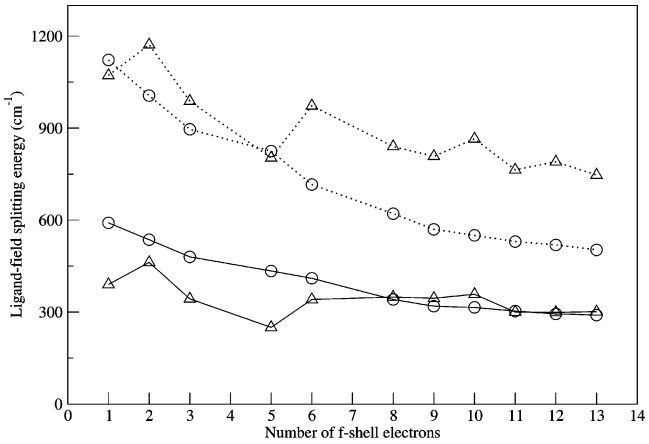

Figure 3. Ligand-field splitting parameters (Δ_1 and Δ_2) in the octahedrally coordinated lanthanide ions in $Cs_2NaLnCl_6$ elpasolites: the splitting energies calculated using effective embedding potential of eq 2 and the observed splitting energies. Calculations were made at the ab initio optimized cation−ligand distances taken from the literature.[63] Solid and dotted lines are used to indicate Δ_1 and Δ_2 parameters, respectively. Triangles and circles are used to guide the eye for experimental[52] and calculated values using KSCED(s) schemes, respectively. The estimated error bars of experimental parameters are not shown because they are of the size of the applied symbols.

The small differences between the KSCED(m) and KSCED(s) results (Δ_1 and Δ_2) for the whole series of embedded lanthanide cations, indicate clearly that lifting the localization assumption does not affect significantly the orbital levels. In some cases, the agreement between the calculated and experimental ligand-field splitting parameters slightly improves. As measured by mean absolute errors in the whole lanthanide series, lifting the localization assumption leads only to a slight deterioration of the calculated splitting energies. It is worthwhile to stress at this point that the intersystem charge-flow possible in KSCED(s) calculations makes the KSCED embedding potential prone to possible flaws of the applied approximations in the relevant functionals.[51] Moreover, the KSCED(s) results approach better the basis set limit for the applied method which is based on the variational principle. The remaining deviations between the KSCED calculated and experimental parameters should be attributed to other assumptions/approximations used in the applied computational scheme: the use of average-of-configurations and approximations for the exchange-correlation- and nonadditive-kinetic-energy potentials.

In the following part, the results were obtained for a number of other elpasolites for which either experimental splitting parameters were not accurately measured yet or do not exist.

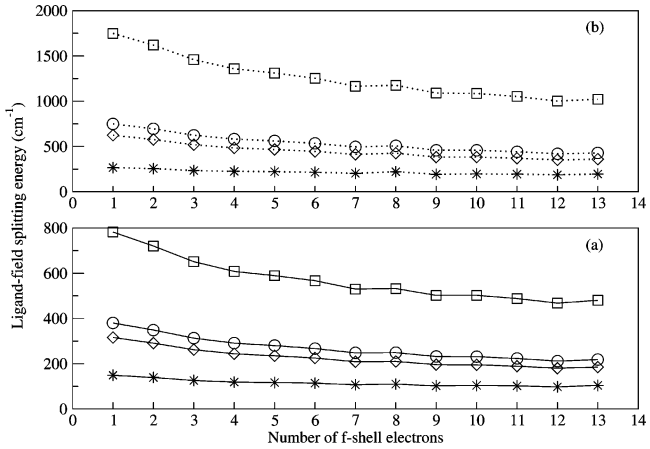

Figure 4. Ligand-field splitting parameters (Δ_1 and Δ_2) in the octahedrally coordinated lanthanide ions for the whole Cs_2NaLnX_6 elpasolites series (X=F, Cl, Br, I) from KSCED(m) calculations using the sum of ionic radii cation−ligand distances.[64] Solid and dotted lines are used to indicate (a) Δ_1 and (b) Δ_2 parameters, respectively. Squares, circles, diamonds, and stars are used to guide the eye for calculated values corresponding to LnF_6^{3-}, $LnCl_6^{3-}$, $LnBr_6^{3-}$, and LnI_6^{3-}, respectively.

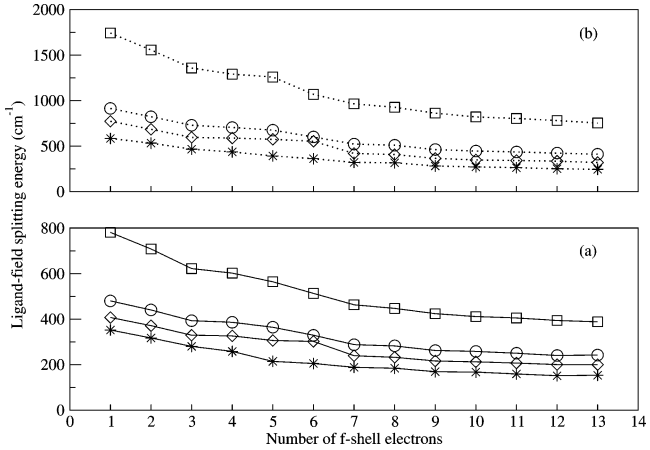

Figure 5. Ligand-field splitting parameters (Δ_1 and Δ_2) in the octahedrally coordinated lanthanide ions for the whole Cs_2NaLnX_6 elpasolites series (X=F, Cl, Br, I) from KSCED(s) calculations using the sum of ionic radii cation−ligand distances.[64] Solid and dotted lines are used to indicate (a) Δ_1 and (b) Δ_2 parameters, respectively. Squares, circles, diamonds, and stars are used to guide the eye for calculated values corresponding to LnF_6^{3-}, $LnCl_6^{3-}$, $LnBr_6^{3-}$, and LnI_6^{3-}, respectively.

Figures 4 and 5 show the calculated values of Δ_1 and Δ_2 for the whole series of Cs_2NaLnX_6 (Tables 3 and 4 collect the corresponding numerical values) derived from either KSCED(m) or KSCED(s) calculations). The ligand-field splitting energies calculated using both techniques increase

Table 3: Ligand-Field Splitting Parameters Δ_1 and Δ_2 (in cm^{-1}) from KSCED(m) Calculations Using the Sum of Ionic Radii Cation−Ligand Distances[64]

	Ce^{3+}	Pr^{3+}	Nd^{3+}	Pm^{3+}	Sm^{3+}	Eu^{3+}	Gd^{3+}	Tb^{3+}	Dy^{3+}	Ho^{3+}	Er^{3+}	Tm^{3+}	Yb^{3+}
						Δ_1							
F^-_6	782	720	651	608	589	567	530	532	502	502	488	468	480
Cl^-_6	380	349	313	291	280	267	248	249	232	231	223	212	218
Br^-_6	316	291	262	244	235	225	209	210	196	195	189	180	185
I^-_6	149	139	126	119	117	114	107	110	102	104	102	98	104
						Δ_2							
F^-_6	1749	1620	1459	1358	1312	1254	1165	1176	1090	1086	1052	1001	1022
Cl^-_6	750	695	624	582	561	534	495	507	459	458	442	420	428
Br^-_6	624	577	519	484	467	445	413	426	383	383	370	352	360
I^-_6	267	256	234	225	222	215	203	221	193	197	194	187	195

Table 4: Ligand-Field Splitting Parameters Δ_1 and Δ_2 (in cm^{-1}) from KSCED(s) Calculations Using the Sum of Ionic Radii Cation−Ligand Distances[64]

	Ce^{3+}	Pr^{3+}	Nd^{3+}	Pm^{3+}	Sm^{3+}	Eu^{3+}	Gd^{3+}	Tb^{3+}	Dy^{3+}	Ho^{3+}	Er^{3+}	Tm^{3+}	Yb^{3+}
						Δ_1							
F^-_6	781	708	622	602	564	513	463	447	424	411	405	394	388
Cl^-_6	480	440	393	386	364	329	288	282	262	258	250	240	242
Br^-_6	407	371	329	326	306	302	239	232	216	212	207	200	200
I^-_6	352	317	280	258	214	205	188	184	169	167	159	151	153
						Δ_2							
F^-_6	1742	1556	1358	1291	1259	1069	965	927	862	821	804	781	754
Cl^-_6	914	823	729	705	676	600	523	510	462	446	436	423	411
Br^-_6	773	685	596	589	575	553	420	407	366	348	342	335	320
I^-_6	584	533	466	437	392	362	321	317	282	272	263	252	245

in the expected order[62] along the series $I^- < Br^- < Cl^- < F^-$. It is worthwhile to note that the ligand−cation (X^-−Ln^{+3}) distance increases along the series F, Cl, Br, and I. Except for iodide elpasolites Cs_2NaLnI_6, the numerical values derived from KSCED(s) and KSCED(m) calculations are very similar. This exceptional behavior of iodide elpasolites Cs_2NaLnI_6 results probably from the fact that iodine has the smallest electron affinity among the considered ligands. In view of the analysis concerning chloroelpasolites, the numerical values derived from KSCED(s) calculations are probably more accurate.

4. Conclusions

In this study, the ligand-field splitting parameters Δ_1 and Δ_2 obtained from orbital-free embedding calculations are reported. To take into account the f-orbital delocalization and the possibility of the ligand ↔ metal charge transfer, supermolecular expansion of basis sets functions was used for each subsystem. The results obtained previously[53] using selected atom-centered functions in the linear combination of atomic orbitals expansion of embedded orbitals (monomolecular expansions for ρ_I and ρ_{II}) are not affected for heavier lanthanides ($f_n > 7$) and are slightly improved for lighter ones ($f_n < 7$) in chloroelpasolites. Our calculations confirm that localizing the cation and ligand orbitals in different regions in space, an intuitive approximation applied in our previous work, is adequate because lifting this assumption does not affect the calculated parameters significantly. Nevertheless, the calculated difference between the t_{1u} and a_{2u} levels (Δ_2 parameter) is underestimated by about 200 cm^{-1} for cations with the f-shell more than half-filled. This underestimation is probably the result of the use of the "average-of-configuration" Ansatz or the inherent errors of the applied approximations for the effective potential in KSCED. The present analysis does not justify a more precise determination of the relative significance of these two effects. Another possible source of deviations between the ligand-field parameters deduced from experiment and the calculated ones might be the result of their strong dependence (r^{-5}−r^{-6}) on the metal−ligand distances. In fact, the actual geometry in the crystal lattice might be different from the standard geometries applied in this work. The current study provides also predictions of the ligand-field splitting parameters for homologous materials: fluoroelpasolites Cs_2NaLnF_6, bromoelpasolites $Cs_2NaLnBr_6$, and iodoelpasolites Cs_2NaLnI_6. The KSCED(s) results are recommended because the additional atom-centered basis functions approach better the complete basis set, whereas their use was found to be numerically stable despite possible flaws in the used approximations for the orbital-free embedding potential given in eq 2.

Acknowledgment. This work is supported by the Swiss National Science Foundation. It is also part of the COST D26 Action.

References

(1) Meyer, G. *Prog. Solid State Chem.* **1982,** *14* (3), 141−219.

(2) Molander, G. A.; Romero, J. A. C. *Chem. Rev.* **2002**, *102*, 2161−2186.

(3) Morss, L. R.; Fuger, J. *Inorg. Chem.* **1969**, *8*, 1433−1439.

(4) Gudel, H. U.; Furrer, A.; Blank, H. *Inorg. Chem.* **1990**, *29*, 4081−4084.

(5) Eldelmann, F. T.; Freckmann, D. M. M.; Schumann, H. *Chem. Rev.* **2002**, *102*, 1851−1896.

(6) Eisenstein, O.; Hitchcock, P. B.; Khvostov, A. V.; Lappert, M. F.; Maron, L.; Perrin, L.; Protchenko, A. V. *J. Am. Chem. Soc.* **2003**, *125*, 10790−10791.

(7) Aparna, K.; Ferguson, M.; Cavell, R. G. *J. Am. Chem. Soc.* **2000**, *122*, 726−727.

(8) Tanner, P. A. *Mol. Phys.* **1985**, *58*, 317−328.

(9) Schwartz, R. W. *Inorg. Chem.* **1977**, *16*, 1694−1697.

(10) Case, D. A.; Lopez, J. P. *J. Chem. Phys.* **1983**, *80*, 3270−3277.

(11) Roser, M. R.; Xu, J.; White, S. J.; Corruccini, L. R. *Phys. Rev. B* **1992**, *45*, 12337−12342.

(12) Eisenstein, O.; Maron, L. *J. Organomet. Chem.* **2002**, *647*, 190−197.

(13) Zhao, C. Y.; Wang, D.; Phillips, D. L. *J. Am. Chem. Soc.* **2003**, *125*, 15200−15209.

(14) Gordon, J. C.; Giesbrecht, G. R.; Clark, D. L.; Hay, P. J.; Koegh, D. W.; Poli, R.; Scott, B. L.; Watkin, J. G. *Organometallics* **2002**, *21*, 4726−4734.

(15) Clark, D. L.; Gordon, J. C.; Hay, P. J.; Martin, R. L.; Poli, R. *Organometallics* **2002**, *21*, 5000−5006.

(16) Cao, X.; Dolg, M. *Mol. Phys.* **2003**, *101*, 2427−2435.

(17) Luo, Y.; Selvam, P.; Ito, Y.; Endou, A.; Kubo, M.; Miyamoto, A. *J. Organomet. Chem.* **2003**, *679*, 84−92.

(18) Jayasankar, C. K.; Richardson, F. S.; Tanner, P. A.; Reid, M. F. *Mol. Phys.* **1987**, *61*, 635−644.

(19) Reid, M. F.; Richardson, F. S.; Tanner, P. A. *Mol. Phys.* **1986**, *60*, 881−886.

(20) Falin, M. L.; Latypov, V. A.; Kazakov, B. N.; Leushin, A. M.; Bill, H.; Lovy, D. *Phys. Rev. B* **2000**, *61*, 9441−9448.

(21) Foster, D. R.; Reid, M. F.; Richardson, F. S. *J. Chem. Phys.* **1985**, *83*, 3225−3233.

(22) Tanner, P. A.; Yulong, L.; Edelstein, N. M.; Murdoch, K. M.; Khaidukov, N. M. *J. Phys.* **1997**, *9*, 7817−7836.

(23) Berry, A. J.; McCaw, C. S.; Morisson, I. D.; Denning, R. G. *J. Lumin.* **1996**, *66*, 272−277.

(24) McCaw, C. S.; Murdoch, K. M.; Denning, R. G. *Mol. Phys.* **2002**, *101*, 427−438.

(25) Denning, R. G.; Berry, A. J.; McCaw, C. S. *Phys. Rev. B* **1997**, *57*, 2021−2024.

(26) Tanner, P. A.; Kumar, V. V. R. K.; Jayasanka, C. K.; Reid, M. F. *J. Alloys Compd.* **1994**, *215*, 349−370.

(27) Tanner, P. A.; Mak, C. S. K.; Edelstein, N. M.; Murdoch, K. M.; Liu, G.; Huang, J.; Seijo, L.; Barandiaran, Z. *J. Am. Chem. Soc.* **2003**, *125*, 13225−13233.

(28) Tanner, P. A.; Mak, C. S. K.; Faucher, M. D. *J. Chem. Phys.* **2001**, *114*, 10860−10871.

(29) Tanner, P. A.; Chua, M.; Reid, M. F. *J. Alloys Compd.* **1995**, *225*, 20−23.

(30) Hohenberg, P.; Kohn, W. *Phys. Rev.* **1964**, *136*, B864−B871.

(31) Kohn, W.; Sham, L. *Phys. Rev.* **1965**, *140*, A1133-A1138.

(32) Jones, R. O.; Gunnarsson, O. *Rev. Mod. Phys.* **1989**, *61*, 689−746.

(33) Jiang, L.; Xu, Q. *J. Phys. Chem. A* **2006**, *110*, 5636−5641.

(34) Yakuphanoglu, F.; Atalay, Y.; Erol, I. *Mol. Phys.* **2005**, *103*, 3309−3314.

(35) Otani, M.; Okada, S.; Oshiyama, A. *Phys. Rev. B* **2003**, *68*, 125424.

(36) Wang, S. G.; Pan, D. K.; Schwarz, W. H. E. *J. Chem. Phys.* **1995**, *102*, 9296−9307.

(37) Forstreuter, J.; Steinbeck, L.; Richter, M.; Eschrig, H. *Phys. Rev. B* **1997**, *55*, 9415−9421.

(38) Said, M.; Zid, F. B.; Bertoni, C. M.; Ossicini, S. *Eur. Phys. J. B* **2001**, *23*, 191−199.

(39) Gutierrez, F.; Rabbe, C.; Poteau, R.; Daudey, J. P. *J. Phys. Chem. A* **2005**, *109*, 4325−4330.

(40) Atanasov, M.; Daul, C.; Gudel, H. U.; Wesolowski, T. A.; Zbiri, M. *Inorg. Chem.* **2005**, *44*, 2954−2963.

(41) Liu, W.; Hong, G.; Dai, D.; Li, L.; Dolg, M. *Theor. Chem. Acc.* **1997**, *96*, 75−83.

(42) Sommerfeld, A.; Welker, H. *Ann. Phys.* **1938**, *32*, 56−65.

(43) Schäffer, C. E. *Mol. Phys.* **1965**, *9*, 401−412.

(44) Urland, W. *Chem. Phys.* **1976**, *14*, 393−401.

(45) Yang, W. *Phys. Rev. Lett.* **1991**, *66*, 1438−1441.

(46) Yang, W. *Phys. Rev. A* **1991**, *44*, 7823−7826.

(47) Cortona, P. *Phys. Rev. B* **1991**, *44*, 8454−8458.

(48) Wesolowski, T. A.; Warshel, A. *J. Chem. Phys.* **1993**, *97*, 8050−8053.

(49) Wesolowski, T. A. *J. Chem. Phys.* **1997**, *106*, 8516−8526.

(50) Kevorkiants, R.; Dulak, M.; Wesolowski, T. A. *J. Chem. Phys.* **2006**, *124*, 024104.

(51) Dulak, M.; Wesolowski, T. A. *J. Chem. Phys.* **2006**, *124*, 164101.

(52) Foster, D. R.; Reid, M. F.; Richardson, F. S. *J. Chem. Phys.* **1985**, *83*, 3813−3830.

(53) Zbiri, M.; Atanasov, M.; Daul, C.; Lastra, J.; Wesolowski, T. A. *Chem. Phys. Lett.* **2004**, *397*, 441−446.

(54) Perdew, J.; Chevary, J.; Vosko, S.; Jackson, K.; Pederson, M.; Singh, D.; Fiolhais, C. *Phys. Rev. B* **1992**, *46*, 6671−6687.

(55) van Leeuwen, R.; Baerends, E. *Phys. Rev. A* **1994**, *49*, 2421−2431.

(56) Wesolowski, T. A.; Weber, J. *Chem. Phys. Lett.* **1996**, *248*, 71−76.

(57) van Lenthe, E.; Snijders, J. G.; Baerends, E. J. *J. Chem. Phys.* **1996**, *105*, 6505−6516.

(58) van Lenthe, E.; van Leeuwen, R.; Baerends, E. J.; Snijders, J. G. *Int. J. Quantum Chem.* **1996**, *57*, 281−293.

(59) Lenthe, E. V.; Baerends, E. J. *J. Comput. Chem.* **2003**, *24*, 1142−1156.

(60) ADF, A. d. f. p. *Theoretical Chemistry*; Vrije Universiteit: Amsterdam, 2005; URL: http://www.scm.com.

(61) te Velde, G.; Bickelhaupt, F. M.; Baerends, E. J.; Guerra, C. F.; van Gisbergen, S. J. A.; Snijders, J. G.; Ziegler, T. *J. Comput. Chem.* **2001**, *22*, 931−967.

(62) Denning, R. G.; Berry, A. J.; McCaw, C. S. *Phys. Rev. B* **1998**, *57* (4), 2021−2024.

(63) Ordejón, B.; Seijo, L.; Barandiarán, Z. *J. Chem. Phys.* **2003**, *119*, 6143−6149.

(64) Shanon, R. D. *Acta Crystallogr. A* **1976**, *32*, 751−767.

CT060035A